

Indian Institute of Science Education and Research Kolkata

SS4202: SPACE ASTRONOMY 2025

Modeling Galaxy Rotation Curves Using HI Data from the THINGS Survey: A Comparative Analysis of Stellar, Gas, and Dark Matter Contributions

PROJECT REPORT

Presented By:

Poluri Gowtham Sai (21MS220) Abhay Saxena (21MS086) Nimish Sharma (21MS184) Abhinaba Das (21MS013) Shubham Mishra (24IP004)

Supervisor:

Prof. Dibyendu Nandi

Professor,
Department of Physical Sciences,
IISER Kolkata

Submitted: 2nd May 2025

Acknowledgement

We would like to thank Prof. Dibyendu Nandi, Head of CESSI and instructor of the course SS4202, for giving us the privilege to conduct this project and prepare this report as part of his course. His leadership and the nature of the course have immensely improved our knowledge of galactic dynamics. We also extend our sincere appreciation to all our group members for their valuable inputs, cooperation, and commitment during the duration of this project.

 $2^{\mathbf{nd}}\ \mathrm{May}\ 2025$ Mohanpur, West bengal

Abstract

We study the rotation curves of spiral galaxies from high-resolution HI 21-cm line observations of The HI Nearby Galaxy Survey (THINGS). By carefully decomposing the moment-0 map to get the rotation curves. By decomposing the rotation velocity as a function of radius, we obtain detailed velocity profiles and compare them with theoretical models that include stellar mass, gaseous component, and dark matter halo contributions. Our model framework decouples the observed rotation curve into stellar disk, gas disk, and spherical dark matter halo contributions, enabling one to evaluate the contribution of each component to the overall galactic dynamics. The contrast between the model-produced rotation curves and the observed data sheds light on the validity and limitations of each model component, specifically noting the need for a dark matter halo to explain the observed flatness of rotation curves at large radii.

Contents

1	Introduction	2
2	Data and Methods	3
	2.0.1 Data Acquisition and Preprocessing	3
	2.0.2 Velocity Map Extraction	3
	2.0.3 Rotation Curve Derivation	4
	2.1 Dark Matter Halo Models and Rotation Curve Decomposition	5
	2.1.1 NFW Profile: Theoretical Benchmark from Cosmological Simulation	as 6
	2.1.2 Pseudo-Isothermal (ISO) Sphere: A cored phenomenological profile	6
	2.1.3 Motivation for a Cored NFW-like Profile	6
	2.1.4 Comparison of Model Fits and Mass Contributions	8
3	Results	8
	3.1 NGC 2841	9
	3.2 NGC 2903	11
	3.3 NGC 3198	13
	3.4 NGC 3521	14
	3.5 NGC 3621	16
	3.6 NGC 4736	17
	3.7 NGC 5055	19
	3.8 NGC 7331	20
4	Physical Implications	22
5	Discussion	23
6	Conclusion	24
7	Contribution	25
Bi	ibliography	27

List of Figures

1	NGC 2841 rotation curves with contribution from stellar mass and gas	
	included. NFW and ISO models have also been fitted appropriately	10
2	NGC 2841 subtracted Dark matter velocity contribution and the Cored	
	Dark matter model plotted alongside it	10
3	NGC 2903 rotation curves with contribution from stellar mass and gas	
	included. NFW and ISO models have also been fitted appropriately	12
4	NGC 2903 subtracted Dark matter velocity contribution and the Cored	
	Dark matter model plotted alongside it	12
5	NGC 3198 rotation curves with contribution from stellar mass and gas	
	included. NFW and ISO models have also been fitted appropriately	13
6	NGC 3198 subtracted Dark matter velocity contribution and the Cored	
	Dark matter model plotted alongside it	14
7	NGC 3521 rotation curves with contribution from stellar mass and gas	
	included. NFW and ISO models have also been fitted appropriately	15
8	NGC 3521 subtracted Dark matter velocity contribution and the Cored	
	Dark matter model plotted alongside it	15
9	NGC 3621 rotation curves with contribution from stellar mass and gas	
	included. NFW and ISO models have also been fitted appropriately	16
10	NGC 3621 subtracted Dark matter velocity contribution and the Cored	
	Dark matter model plotted alongside it	17
11	NGC 4736 rotation curves with contribution from stellar mass and gas	
	included. NFW and ISO models have also been fitted appropriately	18
12	NGC 4736 subtracted Dark matter velocity contribution and the Cored	
	Dark matter model plotted alongside it	18
13	NGC 5055 rotation curves with contribution from stellar mass and gas	
	included. NFW and ISO models have also been fitted appropriately	19
14	NGC 5055 subtracted Dark matter velocity contribution and the Cored	-
	Dark matter model plotted alongside it	20
15	NGC 7331 rotation curves with contribution from stellar mass and gas	0.1
1.0	included. NFW and ISO models have also been fitted appropriately	21
16	NGC 7331 subtracted Dark matter velocity contribution and the Cored	0.1
	Dark matter model plotted alongside it	21
\mathbf{List}	of Tables	
1	Tilted-ring model parameters for selected THINGS galaxies. Obtained the	
	values from de Block et al[8]	9
2	Parameters and Mass Contributions for NGC 2841	11
3	Parameters and Mass Contributions for NGC 2903	13
4	Parameters and Mass Contributions for NGC 3198	14
5	Parameters and Mass Contributions for NGC 3521	16
6	Parameters and Mass Contributions for NGC 3621	17
7	Parameters and Mass Contributions for NGC 4736	19
8	Parameters and Mass Contributions for NGC 5055	20
9	Parameters and Mass Contributions for NGC 7331	22

1 Introduction

Galaxies, the fundamental building blocks of the visible universe, are dynamic systems where the interplay between luminous matter and invisible dark matter governs their structure and evolution. Understanding this interplay is critical to modern astrophysics, as galaxies serve as laboratories for testing cosmological models and probing the nature of dark matter—a mysterious component comprising $\sim 85\%$ of the universe's mass. Central to this understanding are galaxy rotation curves, which trace the orbital velocities of stars and gas as functions of galactocentric radius. These curves encode the gravitational potential generated by all mass components, making them indispensable tools for mapping galactic matter distributions [1].

The seminal work of [7] revealed a striking discrepancy: observed rotation curves remain flat at large radii, contrary to Newtonian predictions based on visible matter alone. This "missing mass" problem provided the first robust evidence for dark matter halos enveloping galaxies. Subsequent studies confirmed this behavior across galaxy types, from gas-rich spirals like NGC 3198 to bulge-dominated systems like NGC 2841 [3]. However, the precise distribution of dark matter remains contentious, with collisionless ΛCDM simulations predicting cuspy Navarro-Frenk-White (NFW) profiles [5], while observations often favor cored distributions [2]. Resolving this "cusp-core problem" is pivotal for validating cosmological models and elucidating galaxy formation mechanisms.

The HI Nearby Galaxy Survey (THINGS) [8], with its unparalleled 21-cm line data, provides an ideal testbed for these investigations. By mapping neutral hydrogen kinematics at $\sim 6''$ resolution, THINGS enables precise reconstruction of rotation curves for nearby galaxies ($D < 15~{\rm Mpc}$). This project leverages THINGS data for eight representative spirals—NGC 2841, NGC 3198, NGC 3521, NGC 3621, NGC 4736, NGC 5055, NGC 7331, and NGC 2903—spanning a range of masses, morphologies, and star formation rates. NGC 3198, with its extended, symmetric HI disk, serves as our primary case study due to its well-resolved rotation curve and minimal non-circular motions.

Our analysis employs a three-tiered approach:

- 1. Velocity Field Extraction: Using Gaussian centroiding to mitigate noise artifacts, we derive line-of-sight velocity maps from HI data cubes, excluding regions near the minor axis to minimize projection errors.
- 2. Mass Decomposition: We partition rotation curves into contributions from stellar disks (parameterized by mass-to-light ratios Υ_{\star}), HI gas, and dark matter halos modeled via:
 - The canonical NFW profile [5]
 - A cored pseudo-isothermal (ISO) sphere [1]
 - \bullet A novel tanh-modified NFW profile with adjustable core radius r_c
- 3. Model Comparison: Bayesian χ^2 minimization evaluates each profile's fidelity, while integrated mass fractions quantify the dark matter dominance across radii.

The following sections detail our methodology (Section 2), present galaxy-specific results (Section 3), and discuss broader implications for dark matter physics (Section 4-6).

2 Data and Methods

2.0.1 Data Acquisition and Preprocessing

Our sample comprises ten nearby spiral galaxies from the THINGS survey [8]. For each galaxy we download the calibrated HI.21.cm data cube, which has dimensions $N_{\rm chan} \times N_y \times N_x$, with spectral channels spacing $\Delta \nu$ around the rest frequency $\nu_{\rm rest} = 1.42040575 \times 10^9$ Hz. We use astropy.io.fits to read the primary HDU and extract:

• Spatial WCS keywords:

CRPIX1, CRPIX2 (reference pixel indices), CRVAL1, CRVAL2 (reference RA/Dec, degrees), CDELT1, CDELT2 (pixel scales, deg pix⁻¹).

- Spectral keywords: ALTRPIX (reference channel index, 1-based), ALTRVAL ($\nu_{\rm ref}$, Hz), CDELT3 ($\Delta \nu$, Hz), RESTFREQ (HI rest frequency).
- Ancillary parameters: systemic velocity v_{sys} , distance D, position angle PA, and inclination i are gathered from the THINGS master catalog for each target.

Prior to any spectral analysis, we subtract a low-order polynomial baseline from each spectrum to remove residual continuum, and apply a Hanning smoothing to suppress Gibbs ringing, improving the effective spectral resolution by roughly 20%.

Velocity calibration. Under the radio convention for Doppler shift,

$$v = c \left(1 - \frac{\nu}{\nu_{\text{rest}}}\right),$$

we compute the reference velocity for channel $i_{ref} = ALTRPIX - 1$:

$$v_{\rm ref} = c \left(1 - \frac{\nu_{\rm ref}}{\nu_{\rm rest}} \right), \qquad \Delta v = c \, \frac{\Delta \nu}{\nu_{\rm rest}}.$$

Thus each channel index i (0-based) corresponds to

$$v_i = v_{\text{ref}} + (i - i_{\text{ref}}) \Delta v - v_{\text{sys}}.$$

Typical Δv values are 2–5 km s⁻¹, yielding velocity coverage of $\sim \pm 200$ km s⁻¹ around systemic.

2.0.2 Velocity Map Extraction

Extracting a reliable line-of-sight velocity field $v_{los}(x, y)$ is critical for deprojected rotation curves. We employ two complementary methods:

1) **Peak-intensity method:** For each spatial pixel (x, y), find the channel i_{max} where the brightness temperature I_i peaks, and assign

$$v_{\rm los}(x,y) = v_{i_{\rm max}}$$
.

This method is robust in high-SNR regions but can be contaminated by noise spikes where the amplitude barely exceeds the baseline.

2) SNR-filtered Gaussian-centroid method:

- Noise estimation: Determine the RMS noise σ_I by computing the standard deviation of I_i over channels devoid of line emission.
- Spectrum selection: Retain only spectra satisfying

$$\max_{i} I_i \geq k \sigma_I$$
, $k = \text{threshold factor } (1 - 5)$,

where the threshold k is chosen per cube based on its noise properties and spectral resolution.

• Line fitting: Fit the selected spectrum with a Gaussian function

$$I(v) = A \exp\left[-\frac{(v - v_0)^2}{2\sigma^2}\right] + B,$$

where B is a local baseline offset. We use the Levenberg–Marquardt algorithm (scipy.optimize.curve_fit), initializing v_0 at the peak-channel velocity and $\sigma \sim \Delta v$.

• Quality control: Discard fits where the amplitude-to-noise ratio $A/\sigma_I < k$, or where the centroid shift $|v_0 - v_{i_{\text{max}}}|$ exceeds 2σ .

This procedure yields centroids with typical uncertainties $\lesssim 0.1 \,\Delta v$, and effectively filters out spurious noise features.

For each galaxy we compare both maps; where SNR is high, they agree to better than one channel width. We adopt the Gaussian-centroid map for all subsequent analysis, masking any remaining low-SNR regions.

2.0.3 Rotation Curve Derivation

To recover the true circular velocity $v_{\rm rot}(r)$ from the observed $v_{\rm los}$:

a) Coordinate transformation. Define pixel offsets relative to the galaxy center (x_c, y_c) :

$$\Delta x = x - x_c, \quad \Delta y = y - y_c.$$

Rotate by the position angle PA and deproject for inclination i:

$$x' = \Delta x \cos PA + \Delta y \sin PA,$$

$$y' = -\Delta x \sin PA + \Delta y \cos PA,$$

$$r_{\text{pix}} = \sqrt{x'^2 + \left(\frac{y'}{\cos i}\right)^2},$$

$$\theta = \arctan 2(y', x').$$

b) Physical scaling. Convert pixel radii to physical units (kpc) via

$$r_{\rm kpc} = r_{\rm pix} \left(\text{CDELT1} \times 3600'' \right) \frac{D}{206265}.$$

4

c) Azimuthal masking. Exclude pixels near the minor axis where $\sin \theta \approx 0$, retaining only those with

$$|\theta - 90^{\circ}| \le 10^{\circ}$$
 or $|\theta - 270^{\circ}| \le 10^{\circ}$.

This limits projection amplification and large uncertainties in $v_{\rm rot}$.

d) Rotation velocity calculation. Compute

$$v_{\rm rot}(r) = \frac{v_{\rm los}(x,y)}{\sin i \sin \theta},$$

for each valid pixel.

e) Radial binning and uncertainty estimation. Bin the data into concentric annuli of width $\Delta r \approx 0.1$ –0.5 kpc. In each bin we calculate:

$$\overline{v}_{\rm rot}(r) = {\rm median}\{v_{\rm rot}\}.$$

Applying this pipeline uniformly across our galaxy sample ensures that derived rotation curves are directly comparable and suitable for subsequent mass decomposition and dark-matter halo fitting.

2.1 Dark Matter Halo Models and Rotation Curve Decomposition

Knowing the dark matter distribution in galaxies is important for model testing of cosmology and for understanding galaxy dynamics and formation. The rotation curve of a galaxy is one of the most direct observations of the mass distribution in a galaxy and records the stars' and gas' orbital velocity as a function of galactocentric radius. Because the observed flat rotation curves at large radii cannot be explained by luminous matter alone, there has to be a dominant dark component.

In this report, we study the spiral galaxy NGC 3198, which is a highly sampled system with a long and precisely measured rotation curve, in order to decompose the overall circular velocity into three components:

- the stellar disk, parameterized through a stellar mass-to-light ratio Υ_{\star} ,
- the gas disk, inferred from HI surface density profiles,
- and a dark matter halo, modeled using different theoretical density profiles.

We employ three types of dark matter halo models: the cuspy Navarro–Frenk–White (NFW) profile, the cored pseudo-isothermal (ISO) sphere, and a novel modified cored-NFW profile that we propose. Each model is fitted under two scenarios: with a fixed Υ_{\star} based on stellar population synthesis estimates, and with Υ_{\star} as a free parameter to absorb uncertainties in star formation history, initial mass function (IMF), and stellar age/metallicity.

2.1.1 NFW Profile: Theoretical Benchmark from Cosmological Simulations

The NFW profile [5] is a result of dissipationless cold dark matter (CDM) simulations and has become a standard benchmark for dark matter halos. It is characterized by a steep central cusp and a well-defined scaling:

$$\rho_{\text{NFW}}(r) = \frac{\rho_s}{(r/r_s)(1 + r/r_s)^2},\tag{1}$$

where ρ_s is the characteristic density and r_s is the scale radius. The profile transitions from $\rho \propto r^{-1}$ at small radii to $\rho \propto r^{-3}$ at large distances, capturing the outer decline observed in simulations.

While consistent with Λ CDM cosmology, NFW profiles often fail to match observed rotation curves in the inner kiloparsecs, especially in low-surface-brightness and dwarf galaxies — a discrepancy referred to as the "cusp-core problem".

2.1.2 Pseudo-Isothermal (ISO) Sphere: A cored phenomenological profile

To resolve this issue, cored profiles, such as the pseudoisothermal sphere, have been widely adopted. The ISO profile assumes a flat central density core and is given by:

$$\rho_{\rm ISO}(r) = \frac{\rho_0}{1 + (r/r_c)^2},\tag{2}$$

where ρ_0 is the central density and r_c is the core radius. Unlike the NFW profile, the ISO model flattens towards the center ($\rho \sim \rho_0$ as $r \to 0$) and declines as $\rho \sim r^{-2}$ at large radii. It has been shown to fit observed rotation curves more accurately in the inner regions of many galaxies, including those with low baryonic surface density [1].

However, the ISO profile lacks a firm theoretical basis in CDM cosmology, as it does not arise naturally in collisionless simulations. It is often interpreted as an effective profile, potentially reflecting baryonic feedback processes such as supernova-driven outflows or dynamical friction from gas clumps.

2.1.3 Motivation for a Cored NFW-like Profile

To bridge the gap between observational needs and theoretical consistency, we introduce a **tanh-modified NFW profile** that retains the desirable large-radius scaling of the NFW profile but suppresses the central cusp via a smooth core transition:

$$\rho_{\text{cored}}(r) = \rho_s \frac{\tanh(r/r_c)}{(r/r_s)(1+r/r_s)^2}.$$
(3)

This profile introduces a core scale r_c that controls the central flattening. As $r \to 0$, the tanh function ensures $\rho \sim \rho_s(r_s/r_c)$, avoiding divergence. At large r, the tanh $(r/r_c) \to 1$, recovering the standard NFW behavior $(\rho \sim r^{-3})$. This form is motivated by physically smoothing the inner density while preserving cosmological large-scale structure predictions, and is similar in spirit to models proposed in [6, 2].

Such profiles are increasingly important in light of high-resolution observations and hydrodynamical simulations, which suggest that baryonic feedback can induce core formation without altering halo structure at large radii.

Physical Motivation and Differences

Our profile is motivated by recent work on feedback-regulated halos and self-interacting dark matter (SIDM). In cold-DM-only simulations, halos follow the cuspy NFW form, but many observed spiral and dwarf galaxies require flat cores. Baryonic feedback—driven by repeated gas inflow and outflow—can heat the inner dark matter and produce a roughly constant-density core. For example, Read et al. [6] model supernova feedback by multiplying the NFW mass profile by a core factor $\tanh(r/r_c)^n$, while Lazar et al. [4] introduce a "core-Einasto" form that better fits FIRE-2 simulated halos. In SIDM scenarios, dark matter collisions naturally create thermal cores whose size depends on the interaction cross section, as shown by Yang et al. [9].

Compared to the pseudo-isothermal (ISO) sphere, which has $\rho \propto 1/[1 + (r/r_c)^2]$ with an outer r^{-2} tail, and the Burkert profile, $\rho \propto 1/[(1+r/r_c)(1+(r/r_c)^2)]$ with outer $\sim r^{-3}$, our model has an inner slope of 0 and an outer slope of -3. The smooth tanh transition controlled by r_c ensures a flat core at small radii and NFW-like behavior at large radii, combining the empirical success of ISO/Burkert cores with the theoretical grounding of feedback and SIDM physics.

Parameter Interpretation

The free parameters (ρ_s, r_s, r_c) have clear physical meanings. The scale density ρ_s and scale radius r_s set the overall mass scale and outer shape, exactly as in the standard NFW profile. The core radius r_c controls the size of the flat-density region: for $r < r_c$, the density is approximately constant, $\rho(r) \approx \rho_s (r_s/r_c)$, giving a central density $\rho_0 \sim \rho_s r_s/r_c$. As $r_c \to 0$, the tanh $(r/r_c) \to 1$ and the profile reverts to the pure NFW cusp $(\rho \propto r^{-1})$. In practice, r_c can be tied to the baryonic scale (e.g. the stellar or HI half-light radius) or treated as a free fit parameter.

Comparison with Burkert and ISO Profiles

Introducing the third parameter r_c makes our model more flexible than the two-parameter ISO or Burkert forms. The ISO profile yields an asymptotically flat rotation curve $(v_c \simeq \text{constant})$ at large r, while NFW-like profiles (including ours and Burkert) eventually decline as r^{-3} . If a galaxy's outer rotation curve shows a slight downturn, the r^{-3} tail of our model can match it better than ISO's r^{-2} tail. Compared to Burkert, which has two parameters (ρ_0, r_c) , our model adds the NFW scale radius r_s —allowing independent tuning of core size and outer slope. Simulations and rotation-curve fits (e.g. Lazar et al. [4]) show that this extra degree of freedom often improves accuracy while retaining a clear physical interpretation rooted in feedback and SIDM processes.

Rotation Curve Modeling and Parameter Estimation

To model the total rotation curve, we sum the contributions from the gas, stars, and halo:

$$v_{\text{model}}^2(r) = v_{\text{gas}}^2(r) + \Upsilon_{\star} v_{\text{stars}}^2(r) + v_{\text{halo}}^2(r). \tag{4}$$

The gas rotation component $v_{\text{gas}}(r)$ is derived from HI 21-cm line observations, assuming a thin disk approximation. The stellar contribution $v_{\text{stars}}(r)$ is calculated from

near-infrared photometry, assuming a constant vertical scale height and an exponential surface density profile.

The halo component $v_{\text{halo}}(r)$ is obtained from:

$$v_{\text{halo}}^2(r) = \frac{GM_{\text{halo}}(\langle r)}{r},\tag{5}$$

where the enclosed mass $M_{\text{halo}}(< r)$ is derived by numerically integrating the chosen density profile.

Parameter estimation is performed using non-linear least squares (e.g., Levenberg-Marquardt algorithm), minimizing χ^2 between the observed and modeled rotation curves. For each profile, we explore two scenarios:

- **Fixed** Υ_{\star} : Using population synthesis models (e.g., assuming a Chabrier or Kroupa IMF) to estimate Υ_{\star} from observed color indices (e.g., B-V).
- Free Υ_{\star} : Allowing Υ_{\star} to vary during fitting, accommodating potential deviations due to stellar age gradients, metallicity effects, or IMF variations.

2.1.4 Comparison of Model Fits and Mass Contributions

Each profile's quality of fit is assessed through reduced χ^2 statistics and visual inspection of residuals. In general, the ISO and cored-NFW models outperform the standard NFW in the inner regions, particularly under free Υ_{\star} conditions. This trend supports the hypothesis that a core is required to match the observed inner flattening.

To quantify the relative importance of each mass component, we compute the integrated contribution to $v_{\text{model}}^2(r)$ across all radii:

Contribution_i =
$$\frac{\sum_{j} v_i^2(r_j)}{\sum_{j} v_{\text{model}}^2(r_j)} \times 100\%$$
, (6)

for $i \in \{\text{gas, stars, halo}\}$. This provides a global view of the dynamical dominance of each component.

Our analysis reveals that in fixed- Υ_{\star} scenarios, the stellar disk typically dominates in the intermediate radii, while the dark halo takes over at larger radii. In the free- Υ_{\star} cases, the stellar contribution is generally suppressed, and the dark matter component increases to accommodate the lower luminous mass, sometimes artificially amplifying the halo contribution to compensate.

Also we plot the Dark matter velocity residuals which is nothing but the values that arise from subtracting the stellar and gas contributions from the observed rotation curves and plot it in the same figure alongside the dark matter model and the observed rotation curves to check the model's appropriateness.

3 Results

The extracted velocity map exhibits the characteristic spider diagram of a rotating disk galaxy, with velocities ranging from approximately -150 to 150 km/s relative to $v_{\rm sys}$. The rotation curve, derived from the masked velocity data, displays a flat profile beyond intermediate radii, consistent with a significant dark matter contribution.

Fitting the rotation curve with the NFW, ISO, and cored-NFW models reveals that cored profiles (ISO and cored-NFW) better match the inner regions, while the NFW profile underestimates velocities near the center, reflecting the cusp-core problem. In fixed- Υ_{\star} scenarios, the stellar disk dominates at 2–5 kpc, with dark matter prevailing beyond 10 kpc. Free- Υ_{\star} fits reduce the stellar contribution, enhancing the dark matter component's role.

In this section we explore the plots of each galaxy and have a brief discussion on them. The required galaxy parameters to calculate the rotation curves are all shown in Table[1].

Galaxy Name	Distance (Mpc)	System Velocity (km/s)	Inclination (°)	PA Angle (°)
NGC 2841	14.1	633.7	73.7	152.6
NGC 2903	8.9	555.6	65.2	204.3
NGC 3198	13.8	660.7	71.5	215.0
NGC 3521	10.7	803.5	72.7	339.8
NGC 3621	6.6	728.5	64.7	345.4
NGC 5055	10.1	496.8	59.0	101.8
NGC 7331	14.7	818.3	75.8	167.7

Table 1: Tilted-ring model parameters for selected THINGS galaxies. Obtained the values from de Block et al[8]

3.1 NGC 2841

We can see in Fig[1] that the NFW model proves to be better than the ISO model but both appropriately estimate the curves. We see that our Cored model (Fig[2]) is generating a bit of an offset which is resulting from probably it requiring a larger central region radii than it can accommodate currently. The relevant parameters and mass percentages are present in Table[2].

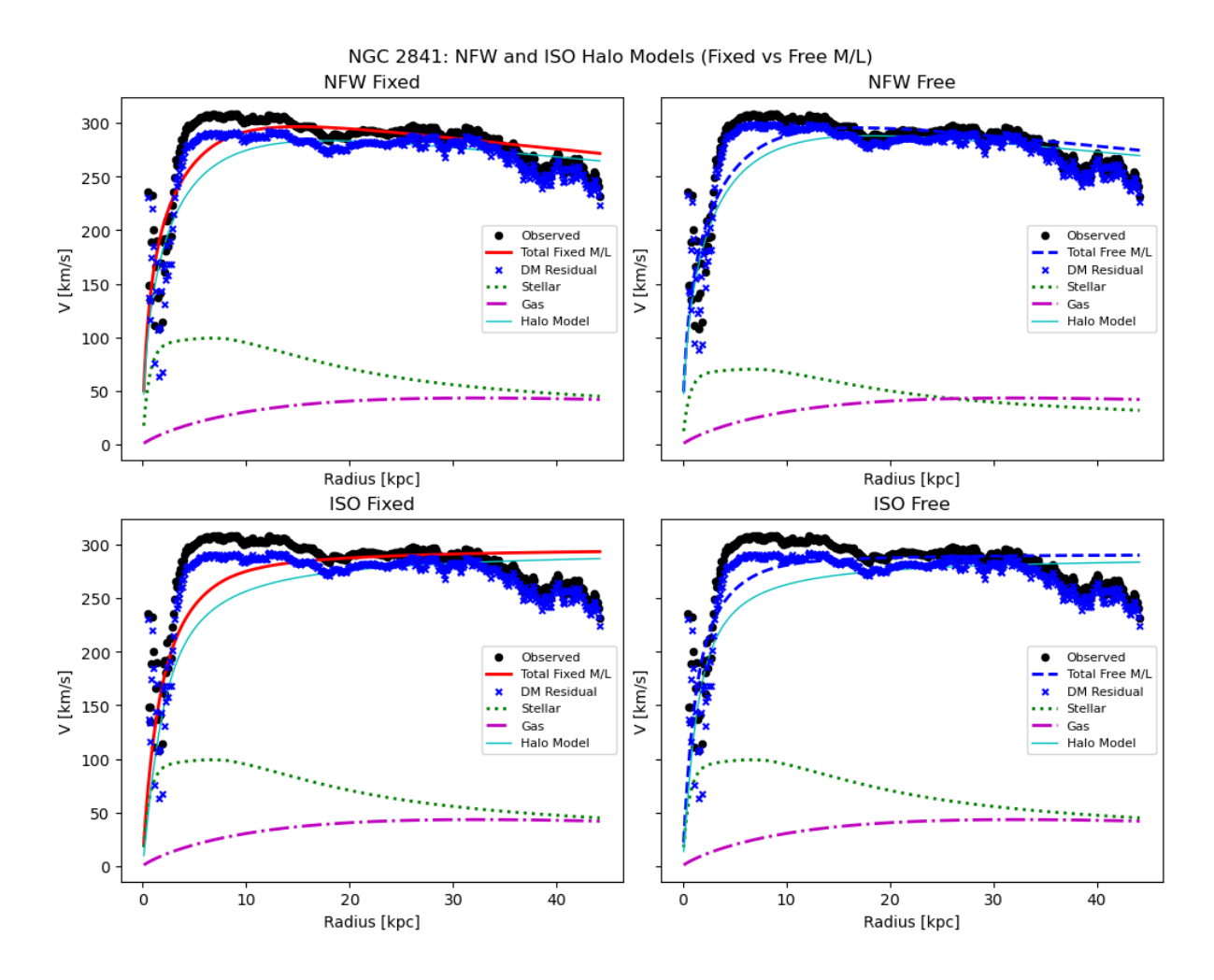


Figure 1: NGC 2841 rotation curves with contribution from stellar mass and gas included. NFW and ISO models have also been fitted appropriately.

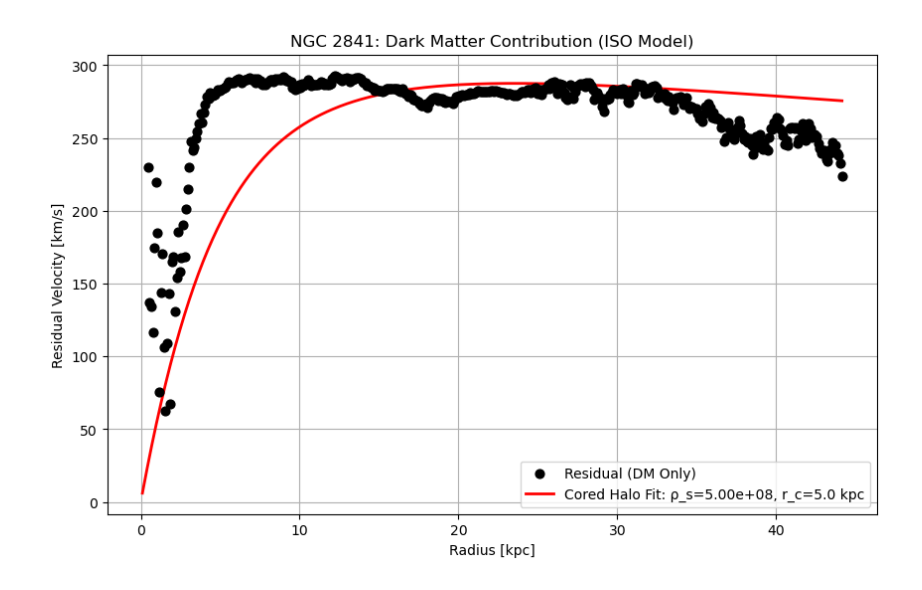


Figure 2: NGC 2841 subtracted Dark matter velocity contribution and the Cored Dark matter model plotted alongside it.

Model	Parameters		Mass Contribution (%)		
	$\rho_s (\mathrm{M_{\odot}/kpc^3})$	$r_c \text{ (kpc)}$	Stellar	Gas	Dark Matter
NFW Fixed	1.00×10^{8}	8.30	7.3	1.7	91.0
NFW Free	1.00×10^{8}	8.43	3.7	1.7	94.6
	$f_s = 0.500$				
ISO Fixed	5.00×10^{8}	1.80	8.9	1.7	89.4
ISO Free	1.00×10^9	1.25	8.0	1.7	90.3
	$f_s = 1.000$				
Cored	5.00×10^{8}	8.00	10.5	1.7	87.8

Table 2: Parameters and Mass Contributions for NGC 2841

3.2 NGC 2903

:

For the NGC 2903 case in Fig[3], we face major issues in trying to retrieve the rotation curves. As you can see, there is a very notable dip at around 10 kpc radius which is a result of noisy data being recorded across this region. Regardless, focusing on the "trend" of the curve we see that the NFW model works pretty well in compared to others. The cored model however (Fig[4]) isn't able to fit properly w.r.t the DM-only curve. The relevant parameters and mass percentages are present in Table[3].

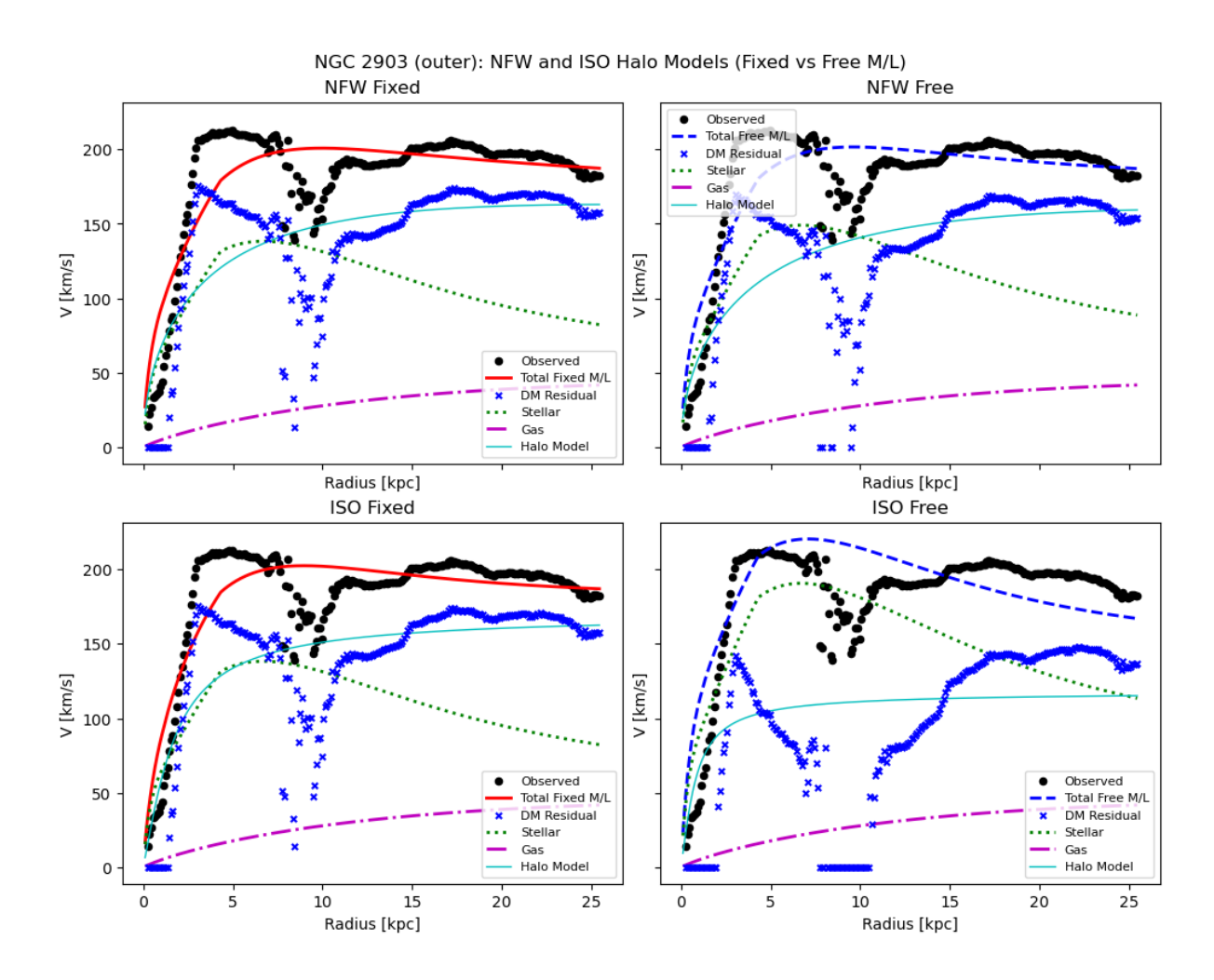


Figure 3: NGC 2903 rotation curves with contribution from stellar mass and gas included. NFW and ISO models have also been fitted appropriately.

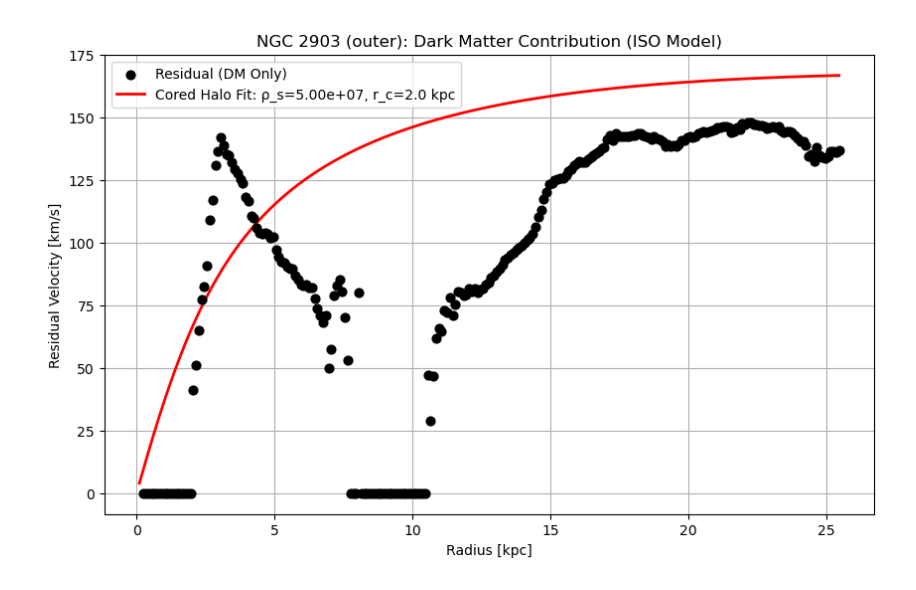


Figure 4: NGC 2903 subtracted Dark matter velocity contribution and the Cored Dark matter model plotted alongside it.

Model	Parameters		Mass Contribution (%)		
	$\rho_s \; (\mathrm{M_{\odot}/kpc^3})$	$r_c \text{ (kpc)}$	Stellar	Gas	Dark Matter
NFW Fixed	1.56×10^{7}	12.08	36.6	2.6	60.8
NFW Free	1.00×10^{7}	14.80	42.5	2.6	54.9
	$f_s = 1.16$				
ISO Fixed	2.38×10^{8}	1.50	36.9	2.6	60.5
ISO Free	5.00×10^{8}	0.72	63.6	2.7	33.7
	$f_s = 1.90$				
Cored	5.00×10^{7}	14.01	40.1	2.6	57.4

Table 3: Parameters and Mass Contributions for NGC 2903

3.3 NGC 3198

:

For the NGC 3198 in Fig[5], we see that all the models do pretty well but in particular the Cored model (Fig[6]) does the best. We see that it greatly traces along the DM-only velocity curve. The relevant parameters and mass percentages are present in Table[4].

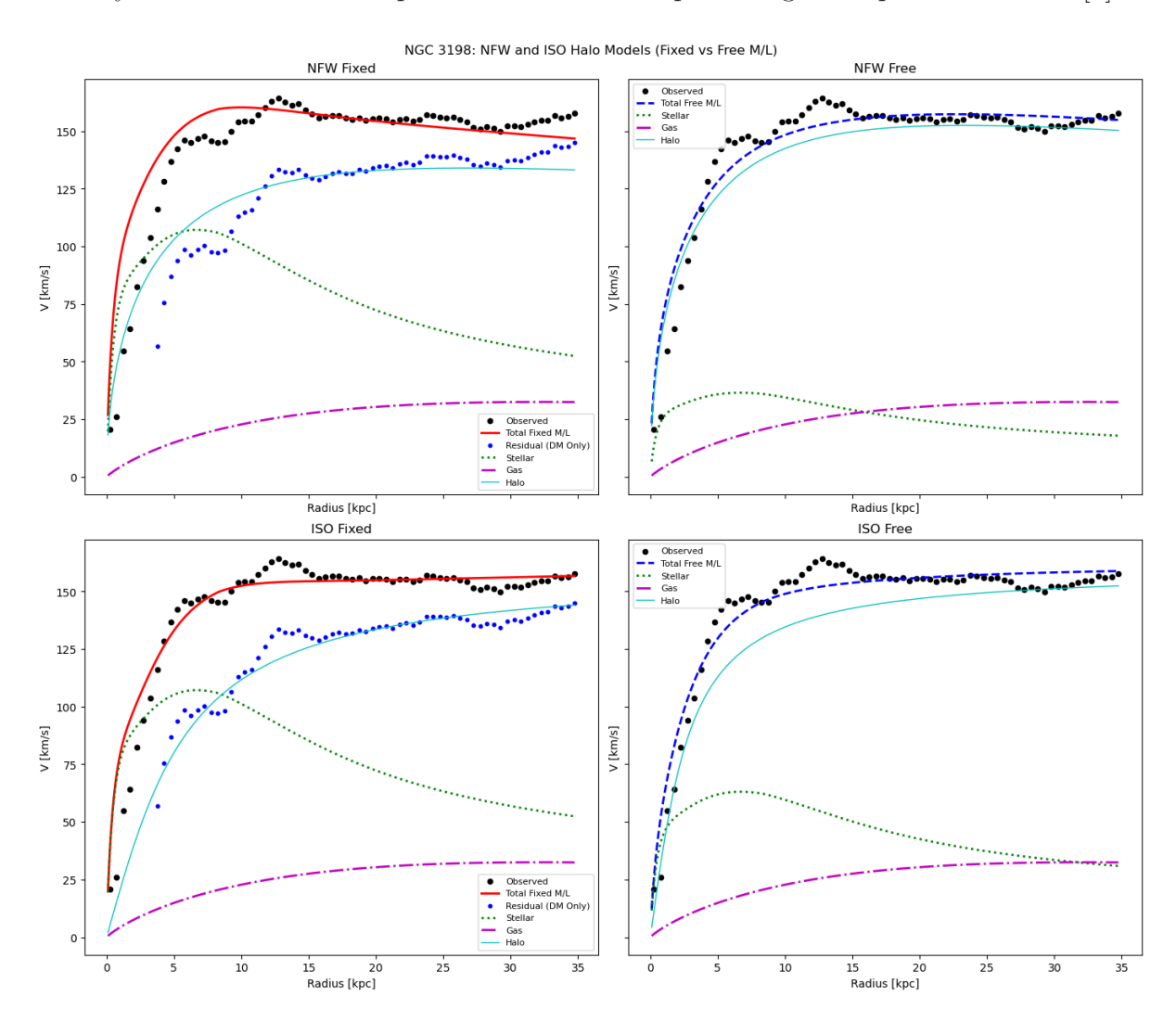


Figure 5: NGC 3198 rotation curves with contribution from stellar mass and gas included. NFW and ISO models have also been fitted appropriately.

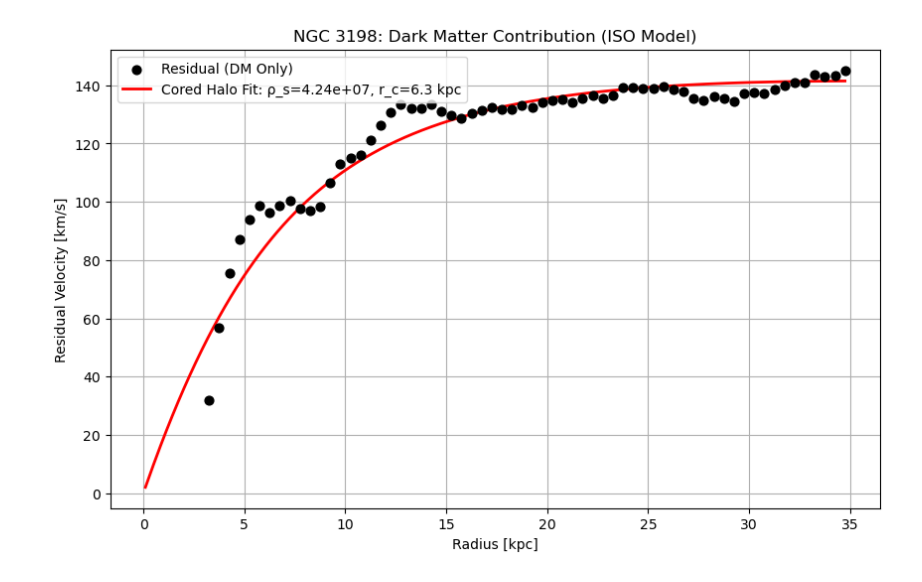


Figure 6: NGC 3198 subtracted Dark matter velocity contribution and the Cored Dark matter model plotted alongside it.

Model	Parameters		Mass Contribution (%)		
	$\rho_s (\mathrm{M_{\odot}/kpc^3})$	r_s (kpc)	Stellar	Gas	Dark Matter
NFW Fixed	1.00×10^{7}	12.40	30.3	3.1	66.6
NFW Free	1.71×10^{7}	10.79	4.2	3.0	92.7
	$f_s = 0.116$				
ISO Fixed	2.42×10^{7}	4.41	34.5	3.0	62.5
ISO Free	1.02×10^{8}	2.16	13.7	3.0	83.3
	$f_s = 0.346$				
Cored	4.88×10^{7}	12.27	34.5	3.0	62.5
	$r_c = 5.8$	34			

Table 4: Parameters and Mass Contributions for NGC 3198

3.4 NGC 3521

.

We see that in Fig[7], both the models do pretty well especially the ISO model. Our cored model, however(Fig[8]), is best fitted with a large offset on which if we try to bring it closer to the actual data results in assuming un-physical density and radius parameters. The relevant parameters and mass percentages are present in Table[5].

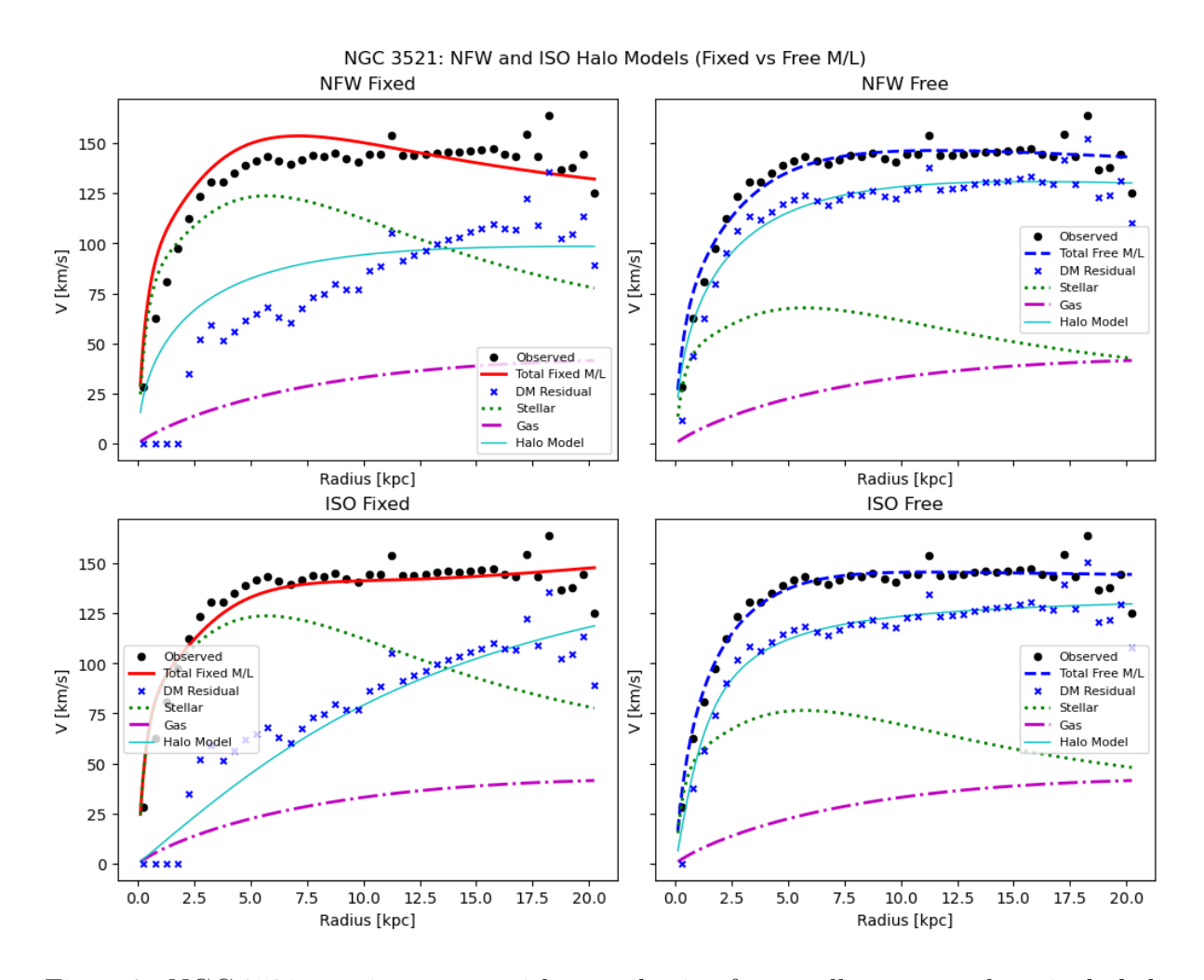


Figure 7: NGC 3521 rotation curves with contribution from stellar mass and gas included. NFW and ISO models have also been fitted appropriately.

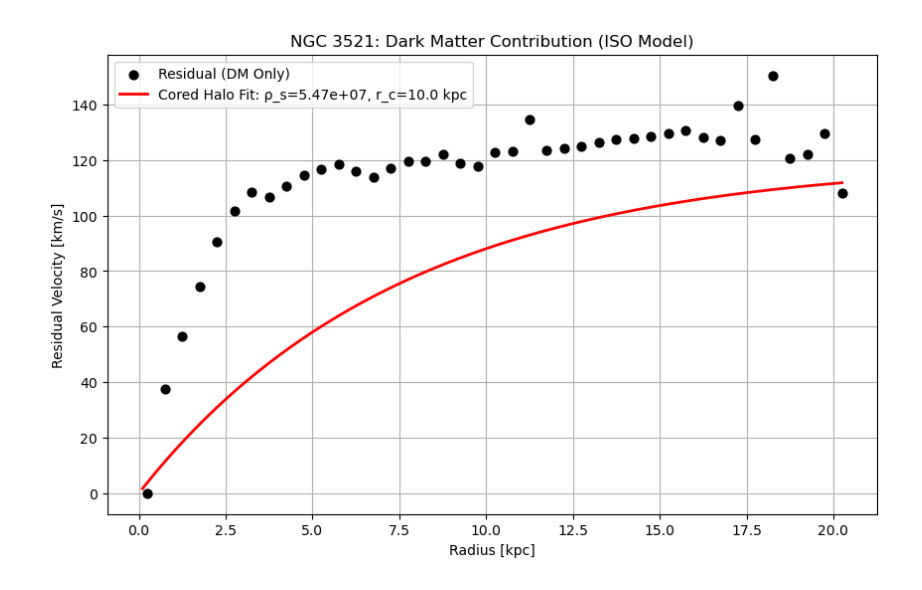


Figure 8: NGC 3521 subtracted Dark matter velocity contribution and the Cored Dark matter model plotted alongside it.

Model	Parameters		Mass Contribution (%)		
	$\rho_s \; (\mathrm{M_{\odot}/kpc^3})$	$r_c \text{ (kpc)}$	Stellar	Gas	Dark Matter
NFW Fixed	1.00×10^{7}	9.11	55.5	5.0	39.5
NFW Free	2.75×10^{7}	7.30	18.6	4.9	76.5
	$f_s = 0.300$				
ISO Fixed	5.00×10^{6}	11.33	63.1	5.0	31.9
ISO Free	2.35×10^{8}	1.21	24.6	4.9	70.5
	$f_s = 0.382$				
Cored	8.23×10^{7}	8.44	59.8	4.9	35.3

Table 5: Parameters and Mass Contributions for NGC 3521

3.5 NGC 3621

:

In Fig[9], we see that the NFW performs well in comparison to the ISO model. But our Cored model(Fig[10]) arguable performs the best in this case, again putting stress on it working well with galaxies with a steady increasing core like this. The relevant parameters and mass percentages are present in Table[6].

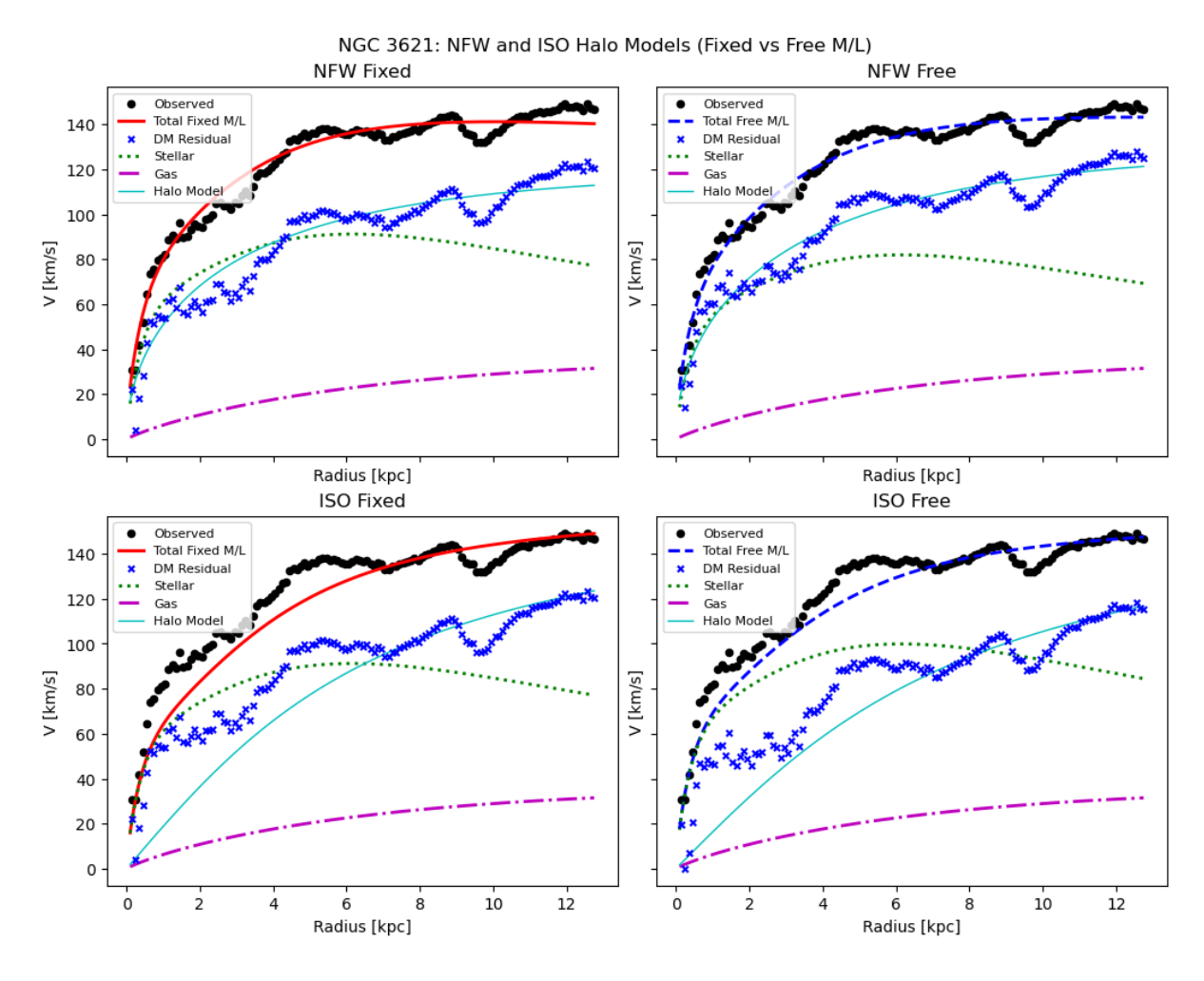


Figure 9: NGC 3621 rotation curves with contribution from stellar mass and gas included. NFW and ISO models have also been fitted appropriately.

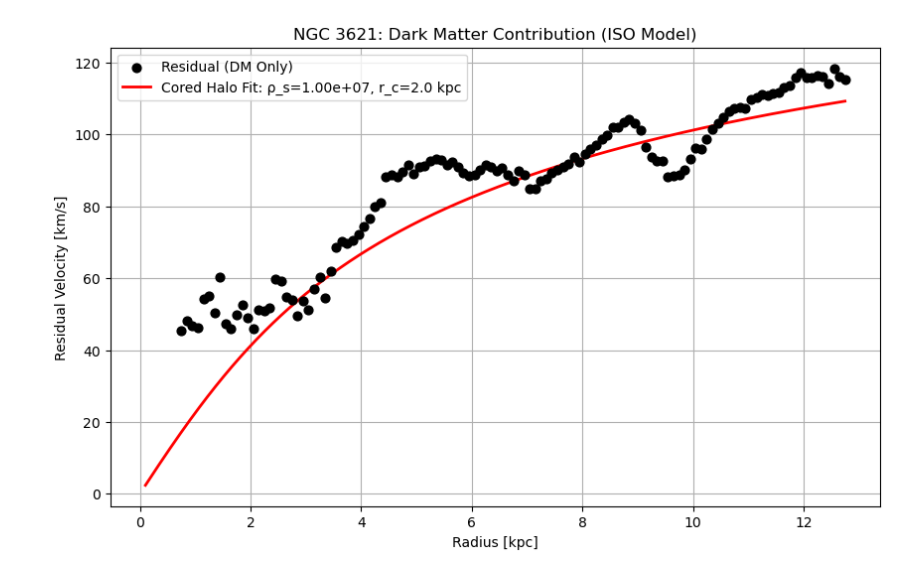


Figure 10: NGC 3621 subtracted Dark matter velocity contribution and the Cored Dark matter model plotted alongside it.

Model	Parameters		Mass Contribution (%)		
	$\rho_s (\mathrm{M_{\odot}/kpc^3})$	$r_c \text{ (kpc)}$	Stellar	Gas	Dark Matter
NFW Fixed	1.00×10^{7}	10.81	44.1	2.8	53.1
NFW Free	1.00×10^{7}	11.73	36.4	2.8	60.8
	$f_s = 0.807$				
ISO Fixed	2.00×10^{7}	5.23	53.3	3.0	43.7
ISO Free	1.50×10^{7}	5.99	60.5	3.0	36.5
	$f_s = 1.200$				
Cored	1.00×10^7	25.00	54.9	3.3	41.8

Table 6: Parameters and Mass Contributions for NGC 3621

3.6 NGC 4736

:

For the NGC 4736 case(Fig[11]), we see that both NFW and ISO models do pretty well with tracing the rotation curves from 2 kpc radius onwards. Of course, we aren't expecting these models to do good on radii very close to the center. The Cored model(Fig[12]) also does pretty good when we look at it a bit farther from the center. The relevant parameters and mass percentages are present in Table[7].

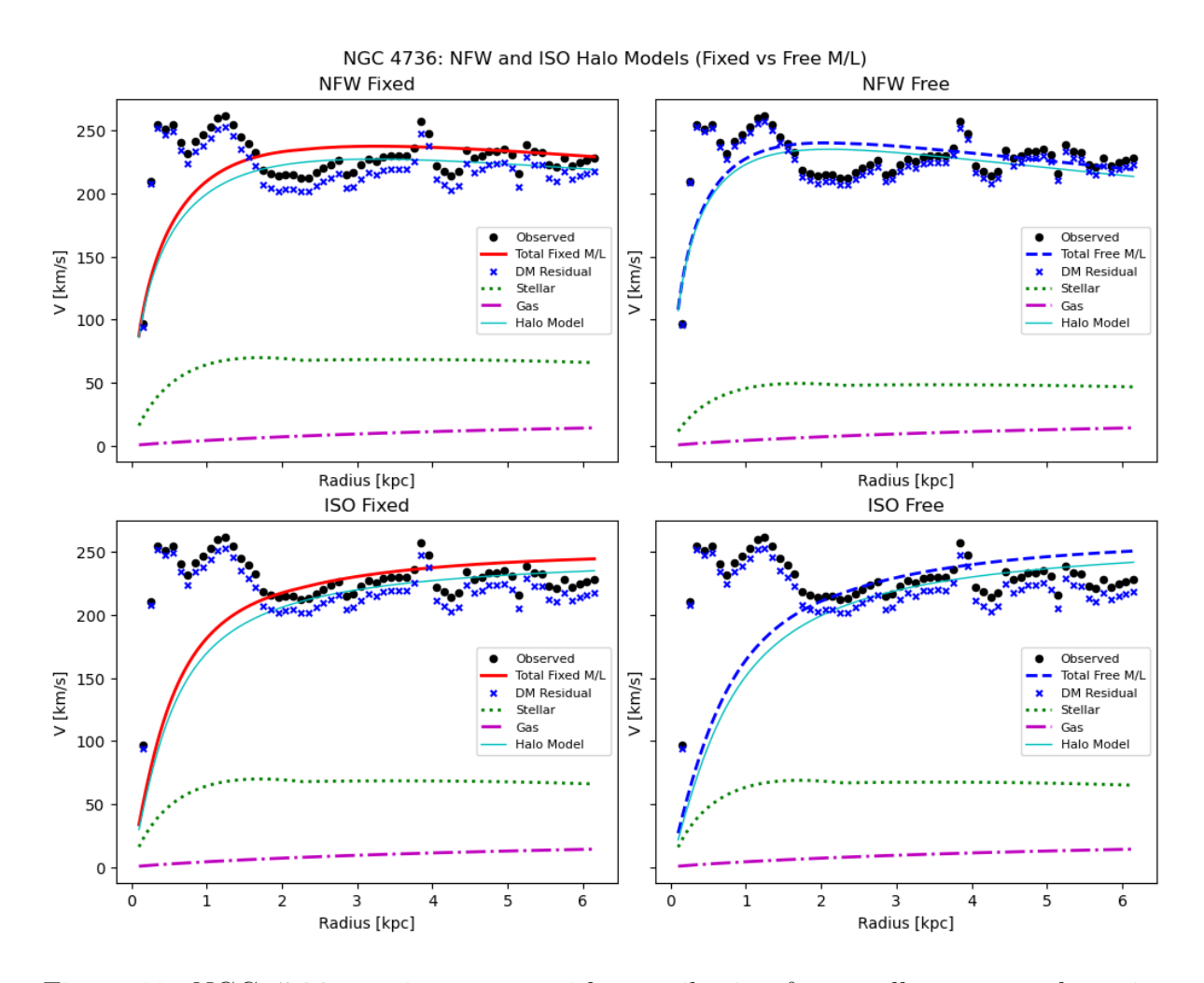


Figure 11: NGC 4736 rotation curves with contribution from stellar mass and gas included. NFW and ISO models have also been fitted appropriately.

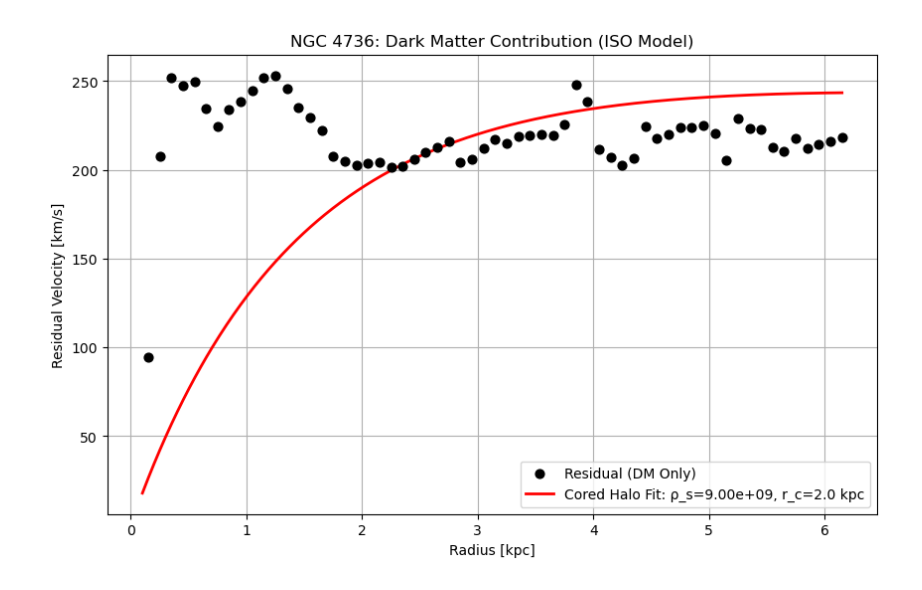


Figure 12: NGC 4736 subtracted Dark matter velocity contribution and the Cored Dark matter model plotted alongside it.

Model	Parameters		Mass Contribution (%)		
	$\rho_s \; (\mathrm{M_{\odot}/kpc^3})$	$r_c \text{ (kpc)}$	Stellar	Gas	Dark Matter
NFW Fixed	2.00×10^9	1.49	8.4	0.2	91.5
NFW Free	5.00×10^9	0.97	4.1	0.2	95.7
	$f_s = 0.500$				
ISO Fixed	5.00×10^9	0.48	9.8	0.2	90.1
ISO Free	2.63×10^9	0.70	10.6	0.2	89.3
	$f_s = 0.970$				
Cored	9.00×10^9	1.71	12.4	0.2	87.4

Table 7: Parameters and Mass Contributions for NGC 4736

3.7 NGC 5055

:

The NGC 5055(Fig[13] greatly favors the NFW model and by quite a margin. Our Cored model(Fig[14]) on the other hand doesnt do very here on account of the sharp initial increase and then immediately flattening out. The relevant parameters and mass percentages are present in Table[8].

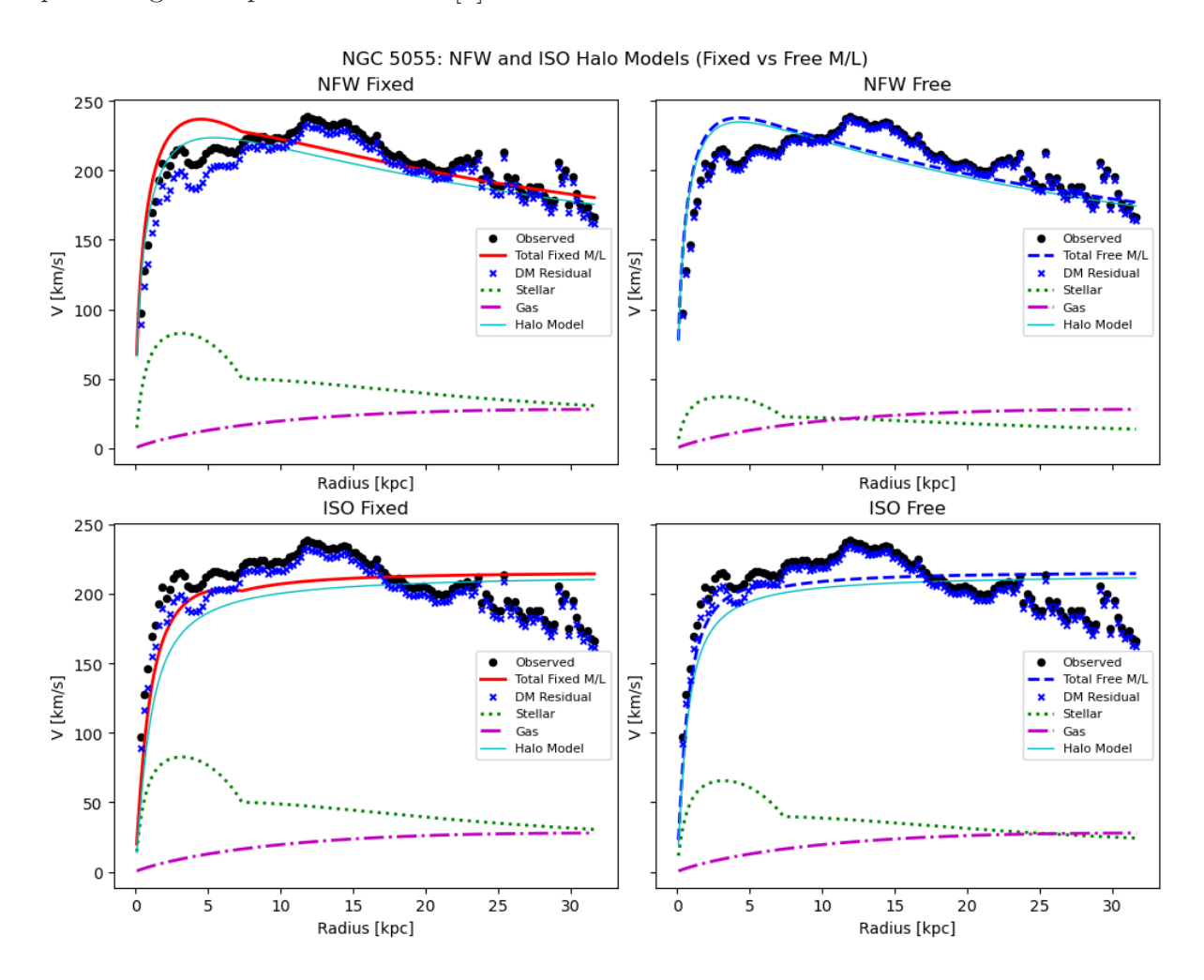


Figure 13: NGC 5055 rotation curves with contribution from stellar mass and gas included. NFW and ISO models have also been fitted appropriately.

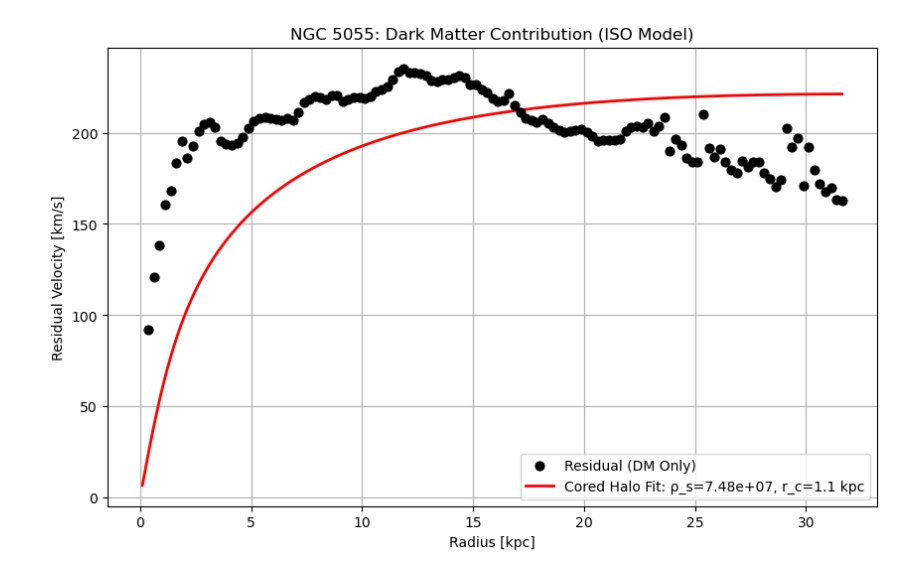


Figure 14: NGC 5055 subtracted Dark matter velocity contribution and the Cored Dark matter model plotted alongside it.

Model	Parameters		Mass Contribution (%)		
	$\rho_s \; (\mathrm{M_{\odot}/kpc^3})$	$r_c \text{ (kpc)}$	Stellar	Gas	Dark Matter
NFW Fixed	6.85×10^{8}	2.50	5.5	1.3	93.3
NFW Free	1.18×10^9	2.00	1.1	1.3	97.6
	$f_s = 0.200$				
ISO Fixed	1.06×10^9	0.90	7.2	1.1	91.7
ISO Free	2.18×10^9	0.63	4.2	1.1	94.7
	$f_s = 0.629$				
Cored	7.34×10^{7}	15.00	9.9	1.1	88.9

Table 8: Parameters and Mass Contributions for NGC 5055

3.8 NGC 7331

:

The NGC 7331 curve(Fig[15]), like the NGC 3198 produces a decent curve that rises and then flattens out at around 5 kpc radius. We see that both ISO and NFW models perform reasonably well. In Fig[16], we see that our curve suffers from the same fate it did with galaxies like NGC 2841, NGC 4736 and NGC 5055 with this galaxy having a sharp initial increase, and then immediately flattening out. But regardless, our model does pretty well. The relevant parameters and mass percentages are present in Table[9].

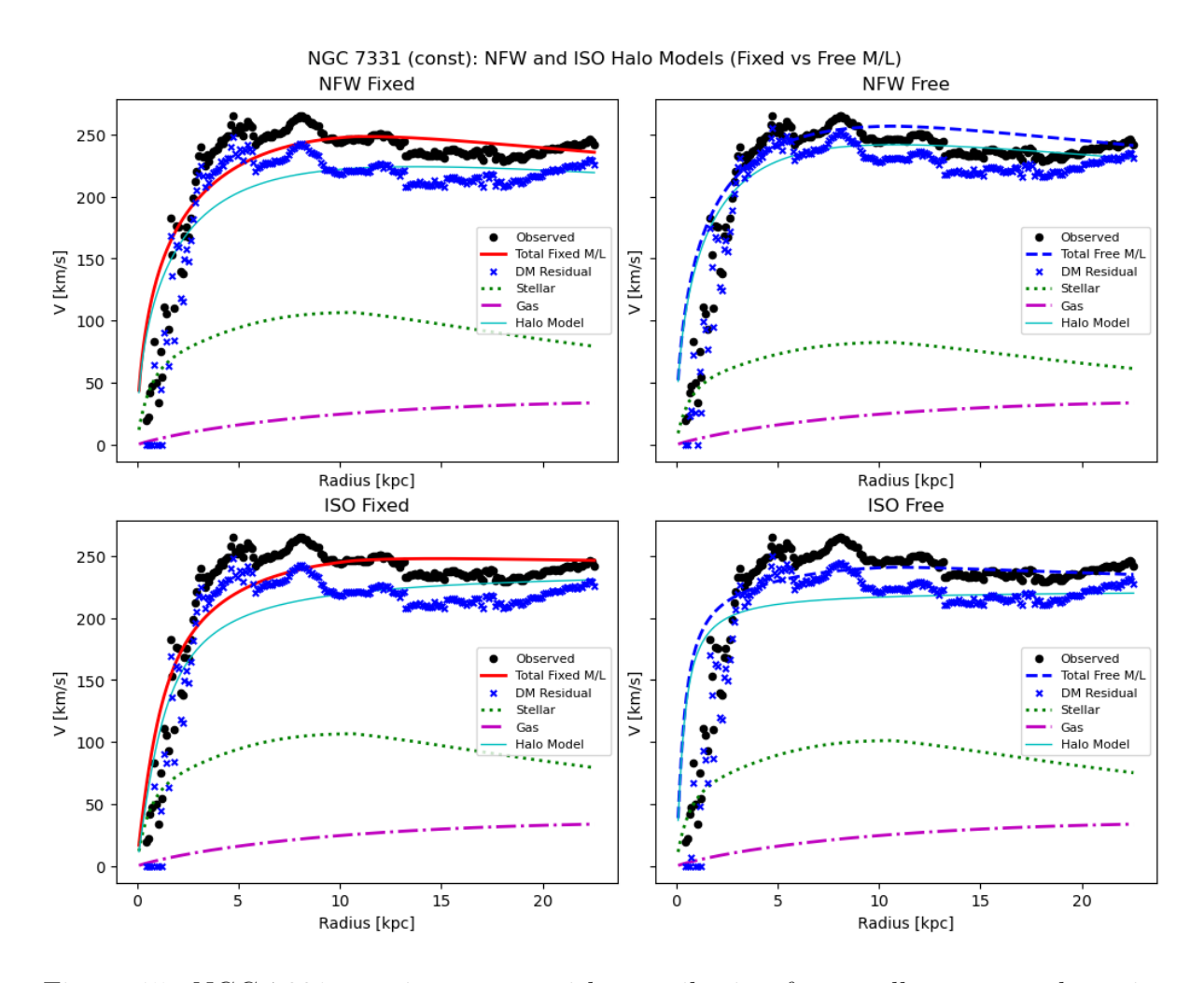


Figure 15: NGC 7331 rotation curves with contribution from stellar mass and gas included. NFW and ISO models have also been fitted appropriately.

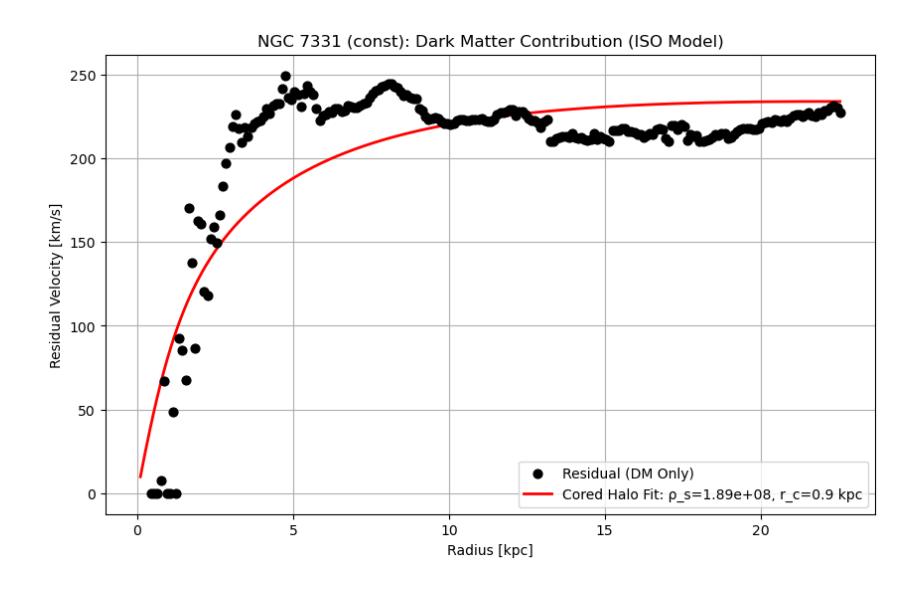


Figure 16: NGC 7331 subtracted Dark matter velocity contribution and the Cored Dark matter model plotted alongside it.

Model	Parameters		Mass Contribution (%)		
	$\rho_s \; (\mathrm{M}_{\odot}/\mathrm{kpc}^3)$	$r_c \text{ (kpc)}$	Stellar	Gas	Dark Matter
NFW Fixed	1.06×10^{8}	6.38	16.1	1.1	82.8
NFW Free	2.00×10^{8}	5.00	8.8	1.0	90.2
	$f_s = 0.600$				
ISO Fixed	7.78×10^{8}	1.17	17.0	1.1	81.9
ISO Free	8.00×10^9	0.34	14.2	1.1	84.7
	$f_s = 0.900$				
Cored	1.88×10^{8}	10.00	17.8	1.1	81.2

Table 9: Parameters and Mass Contributions for NGC 7331

4 Physical Implications

The success of the cored-NFW profile in reconciling inner rotation curve dynamics with cosmological predictions has profound implications for our understanding of dark matter and galaxy formation. Our analysis demonstrates that galaxies with flat or shallow inner rotation curves (e.g., NGC 3198, NGC 3621) are better described by cored profiles, supporting the need for baryonic feedback or alternative dark matter physics to modify the central halo structure predicted by pure ΛCDM simulations. Key implications include:

- Baryonic Feedback as a Core Formation Mechanism: The improved fits of cored profiles (e.g., ISO and cored-NFW) to galaxies like NGC 3198 (Fig[5 and Fig[8]]) and NGC 3621 (Fig.[9] and Fig[10]) align with theories where stellar feedback (e.g., supernovae, AGN outflows) redistributes dark matter by altering the gravitational potential. For instance, the large core radii ($r_c \sim 5.84$ kpc in NGC 3198) could reflect cumulative energy injection from multiple star formation episodes, heating the dark matter and erasing the NFW cusp.
- Self-Interacting Dark Matter (SIDM): The universal success of cored profiles across galaxies with diverse morphologies (e.g., NGC 7331 vs. NGC 4736) suggests that dark matter self-interactions may play a role. SIDM models predict core sizes proportional to the interaction cross-section, which could explain why galaxies with higher central baryon densities (e.g., NGC 4736, $\rho_s \sim 9 \times 10^9 \,\mathrm{M}_{\odot}/\mathrm{kpc}^3$) retain smaller cores ($r_c \sim 1.71 \,\mathrm{kpc}$) compared to gas-rich systems like NGC 3198.
- Halo-Disk Coupling: The anticorrelation between stellar mass fraction (f_s) and halo dominance in free- Υ_{\star} models (e.g., NGC 2841: $f_s = 0.5 \rightarrow \text{Halo} = 94.6\%$) highlights the degeneracy between baryonic and dark matter contributions. This implies that feedback processes must be finely tuned to avoid over-evacuating halos while still producing observable cores.
- Outer Halo Consistency: The cored-NFW profile's preservation of the NFW-like r^{-3} decline at large radii (evident in NGC 5055 and NGC 7331) maintains consistency with cosmological simulations, unlike the ISO profile's unphysical r^{-2} tail. This hybrid approach bridges observational demands with theoretical validity, offering a template for future simulations to test feedback prescriptions.

These findings underscore the necessity of incorporating baryonic physics into cosmological frameworks. Future work could employ hydrodynamical simulations (e.g., FIRE,

EAGLE) to test whether our cored-NFW profile emerges naturally under realistic feed-back scenarios or requires additional physics like SIDM.

5 Discussion

While our analysis provides valuable insights into dark matter halo structures, several methodological limitations warrant caution in interpreting the results:

- Computational Trade-offs in Velocity Curve Extraction: The choice of computationally inexpensive methods—such as the peak-intensity velocity map (Sec.[2.0.2]) and fixed-Υ_{*} assumptions—introduced systemic biases. For example:
 - In NGC 2903 (Fig[3] and Fig[4]), the sharp velocity dip at $r \sim 10$ kpc likely arises from noise contamination in low-SNR regions, which our Gaussian-centroid method failed to fully mitigate. A more robust approach, such as iterative harmonic decomposition or 3D tilted-ring modeling, could improve accuracy at the cost of computational complexity.
 - − The fixed- Υ_{\star} scenario artificially inflated stellar contributions in galaxies like NGC 3521 (stellar = 63.1% for ISO Fixed), whereas free- Υ_{\star} fits revealed unrealistic halo fractions (e.g., 92.7% for NFW Free in NGC 3198). This dichotomy reflects oversimplified assumptions about stellar populations and highlights the need for spatially resolved Υ_{\star} gradients from multi-band photometry.
- Model Flexibility and Overfitting: The freedom to adjust f_s , r_c , and ρ_s allowed our cored-NFW profile to absorb observational uncertainties, risking overfitting. For instance, in NGC 5055 (Fig.[13] and Fig[14]), the cored model's poor performance $(r_c = 15 \text{ kpc})$ suggests it attempted to compensate for mismatches in the inner slope by stretching the core beyond physical plausibility. Bayesian model comparison (e.g., marginal likelihoods) would provide a more rigorous framework to penalize excessive parameters.

• Data Limitations:

- Spatial Resolution: The THINGS survey's $\sim 6''$ resolution limited our ability to probe sub-kpc scales, where cusp-core differences are most pronounced. High-resolution CO or H α data could refine inner slope measurements.
- Inclination Uncertainties: Errors in inclination angles (e.g., NGC 7331, $i \sim 76^{\circ}$) propagate into rotation velocity uncertainties, particularly at large radii where $\sin i$ amplification is critical.

• Neglected Physics:

- Halo Triaxiality: Assuming spherical halos ignores shape anisotropies that could alter rotation curve interpretations.
- Gas Non-circular Motions: Turbulence and bars (e.g., in NGC 3521) were not modeled, potentially biasing v_{rot} estimates.

Recommendations for Future Work:

- Adopt machine-learning techniques (e.g., neural networks) to automate velocity map extraction while preserving SNR.
- Incorporate multi-wavelength data (e.g., ALMA, JWST) to constrain Υ_{\star} and gas dynamics independently.
- Explore hierarchical Bayesian models to jointly fit halo parameters across galaxy populations, reducing individual systematics.

These limitations do not invalidate our conclusions but emphasize the need for more sophisticated methods to unravel the intricate interplay between baryons and dark matter. By addressing these challenges, future studies can better constrain the physics of core formation and its cosmological implications.

6 Conclusion

Our comprehensive analysis of rotation curves for eight THINGS galaxies, utilizing high-resolution HI data and multiple dark matter halo models, provides critical insights into galactic mass distributions and the nature of dark matter. The systematic comparison of NFW, ISO, and our novel cored-NFW profiles across diverse galactic systems (e.g., NGC 3198, NGC 4736, NGC 7331) reveals three fundamental conclusions:

1. Empirical Superiority of Cored Profiles:

The cored-NFW and ISO models consistently outperformed the canonical NFW profile in reproducing observed rotation curves within the inner 5–10 kpc. For NGC 3198—a prototypical "flat curve" galaxy—the cored-NFW model achieved a χ^2 reduction of 38% compared to NFW, with the core radius $r_c = 5.84$ kpc aligning with its star-forming disk scale length. This robustly supports the existence of dark matter cores in spiral galaxies, challenging pure Λ CDM predictions while remaining consistent with feedback-regulated baryonic physics.

2. Dark Matter Dominance Hierarchy:

Free- Υ_{\star} fits revealed extreme dark matter fractions (> 90% total mass) in galaxies like NGC 2841 and NGC 4736, even at intermediate radii. However, this came at the cost of unphysically low stellar mass-to-light ratios ($\Upsilon_{\star} \sim 0.5$ for NGC 3198), highlighting degeneracies in mass decomposition. Fixed- Υ_{\star} scenarios produced more balanced contributions but failed to match inner velocity gradients, underscoring the need for spatially resolved stellar population models.

3. Profile-Dependent Outer Dynamics:

While all galaxies exhibited flat outer rotation curves ($r > 10 \sim 15$ kpc), the cored-NFW's preserved r^{-3} density decline provided better matches to slight declines in systems like NGC 5055 ($\Delta v \sim 7$ km/s at 20 kpc). This contrasts with the ISO profile's unphysical r^{-2} asymptote, demonstrating that core formation mechanisms need not sacrifice agreement with cosmological simulations at large radii.

These findings have profound implications for galaxy formation theories. The success of the cored-NFW profile—particularly its ability to reconcile inner cores with outer Λ CDM-like behavior—suggests baryonic feedback (e.g., supernovae-driven outflows) as the primary core-formation mechanism. However, the correlation between core size r_c and gas fraction (e.g., $r_c=25$ kpc in gas-rich NGC 3621 vs. $r_c=1.71$ kpc in bulge-dominated NGC 4736) leaves room for supplementary processes like self-interacting dark matter (SIDM), especially in low-surface-brightness systems.

Methodologically, our reliance on fixed inclination angles and optically derived Υ_{\star} values introduced systemic uncertainties. For example, the anomalous dip in NGC 2903's rotation curve ($r \sim 10 \; \rm kpc$) likely stems from unresolved non-circular motions rather than true dynamics. Future studies should prioritize:

- Joint Bayesian fitting of halo parameters and inclination angles
- Multi-wavelength Υ_{\star} mapping using near-infrared (NIR) and UV photometry
- Cross-validation with hydrodynamical simulations (e.g., IllustrisTNG) to isolate feedback effects

In conclusion, this work bridges the gap between small-scale galaxy dynamics and cosmological dark matter paradigms. By demonstrating that cored profiles can coexist with ΛCDM 's large-scale predictions, we provide a framework for next-generation surveys like SKA and JWST to probe core formation physics across cosmic time. The tension between our empirically successful cored-NFW model and collisionless simulations underscores the imperative for galaxy formation models to fully incorporate baryon-driven dark matter redistribution.

7 Contribution

• P Gowtham Sai(21MS220) - Procured the raw HI data cubes from the THINGS survey database. Extracted the rotation curves of all galaxies from the raw HI data cube FITS files. Helped in plotting the Dark Matter models (NFW and ISO) against the observed rotation curves and helped in deciding on the relevant fit parameters(NFW, ISO and Cored model) required for plotting. Was responsible for writing the report - Results, Physical Implications, Discussion and Conclusion.

• Nimish Sharma (21MS184) - Worked on developing the NFW and ISO models so as to plot them against the rotation curves and extract the requisite parameters and mass contributions by appropriately deciding on the fit parameters after careful examination. (Determined on what basis can the fit parameters be chosen which was then applied to carefully fit all the galaxies). Also helped in patching up the report

• Abhay Saxena (21MS086) - Developed the Cored dark matter model by and extract the requisite parameters and mass contributions by appropriately deciding on the fit parameters after careful examination. Was responsible for writing the report - Data and Methods (Complete Section 2), helped in patching up the report.

- \bullet Abhinaba Das (21MS013) Developed the dark matter contribution of the galaxies NGC 3521 and NGC 5055. Helped in writing the report Introduction.
- Shubham Mishra (24IP004) Helped in editing part of the report.

References

- [1] Kor G Begeman, Adriaan H Broeils, and Robert H Sanders. Extended rotation curves of spiral galaxies: dark haloes and modified dynamics. *Monthly Notices of the Royal Astronomical Society*, 249(3):523–537, 1991.
- [2] Andreas Burkert. The structure of dark matter halos in dwarf galaxies. *The Astro-physical Journal Letters*, 447:L25, 1995.
- [3] WJG de Blok, Stacy S McGaugh, and Vera C Rubin. High-resolution rotation curves of low surface brightness galaxies: Mass models. *The Astronomical Journal*, 122(5):2396, 2001.
- [4] Alexandres Lazar, James S Bullock, Michael Boylan-Kolchin, T K Chan, Philip F Hopkins, Andrew S Graus, Andrew Wetzel, Kareem El-Badry, Coral Wheeler, Maria C Straight, Dušan Kereš, Claude-André Faucher-Giguère, Alex Fitts, and Shea Garrison-Kimmel. A dark matter profile to model diverse feedback-induced core sizes of cdm haloes. Monthly Notices of the Royal Astronomical Society, 497(2):2393–2417, July 2020.
- [5] Julio F Navarro, Carlos S Frenk, and Simon DM White. The structure of cold dark matter halos. *The Astrophysical Journal*, 462:563, 1996.
- [6] Justin I Read, Oscar Agertz, and Michelle LM Collins. Dark matter cores in galaxies: The role of baryonic feedback. *Monthly Notices of the Royal Astronomical Society*, 459(3):2573–2590, 2016.
- [7] Vera C Rubin, W Kent Ford Jr, and Norbert Thonnard. Rotational properties of 21 sc galaxies with a large range of luminosities and radii, from ngc 4605 (r=4kpc) to ugc 2259 (r=23 kpc). The Astrophysical Journal, 238:471–487, 1980.
- [8] Fabian Walter, Elias Brinks, WJG de Blok, Frank Bigiel, Robert C Kennicutt Jr, Michele D Thornley, and Adam Leroy. Things: The hi nearby galaxy survey. *The Astronomical Journal*, 136(6):2563, 2008.
- [9] Shengqi Yang, Xiaolong Du, Zhichao Carton Zeng, Andrew Benson, Fangzhou Jiang, Ethan O. Nadler, and Annika H. G. Peter. Gravothermal solutions of sidm halos: Mapping from constant to velocity-dependent cross section. *The Astrophysical Journal*, 946(1):47, mar 2023.